

Formation mechanism of a faceted interface: *In situ* observation of the Si(100) crystal-melt interface during crystal growth

M. Tokairin,* K. Fujiwara, K. Kutsukake, N. Usami, and K. Nakajima

Institute for Materials Research (IMR), Tohoku University, Katahira 2-1-1, Aoba-ku, Sendai 980-8577, Japan

(Received 24 September 2009; published 12 November 2009)

We investigated the formation mechanism of a faceted crystal-melt interface by *in situ* observation. It was directly proved that a wavy perturbation is introduced into a planar crystal-melt interface and the perturbation results in zigzag facets. Such a facet formation process was observed when growth velocity was high, although planar interfaces were maintained at low growth velocities. It was shown by theoretical analysis that the negative temperature gradient generated by the latent heat of crystallization at high growth velocities amplifies the perturbation and leads to the facet formation.

DOI: 10.1103/PhysRevB.80.174108

PACS number(s): 81.10.Aj

I. INTRODUCTION

Semiconductors, semimetals, and some organic compounds exhibit faceted crystal-melt interfaces during crystallization processes, in contrast to metals, which exhibit planar, cellular, or dendritic growth.¹⁻³ Jackson considered that this difference is based on the degree of surface roughness on the atomic scale and successfully predicted whether a material exhibits a faceted interface using the α factor.^{4,5} However, there has not been clear explanation of how faceted interface is formed during crystal growth.

The faceted crystal-melt interface of Si has attracted many researchers because Si crystals are widely used in semiconductor devices. It is known that the Si(100) crystal-melt interface is atomically rough, and thus, zigzag facets surrounded by the most stable {111} habit planes are formed at the interface.⁶⁻¹² Landman *et al.*^{6,7} conducted molecular-dynamics simulations and indicated that atomic-scale facets are formed on the Si(100) crystal-melt interface. It is also known that the scale of such zigzag facets changes during crystal growth.¹³⁻¹⁹ Pfeiffer *et al.* concluded that the scale of facets changes owing to the loss of short facets and the generation of new facets, from the results of their observation of recrystallized Si films and computer simulation.¹⁵ Thus, one possible faceting model is that atomic-scale facets are formed first and gradually enlarge to macroscopic facets.^{15,16} However, the formation mechanism of the faceted interface is still obscure. To answer this question, the *in situ* observation of facet formation is necessary.

In this study, we directly observed the formation of zigzag facets at the Si(100) crystal-melt interface during crystal growth. As a result, it was clearly shown that a wavy perturbation is introduced into a planar interface, and the perturbation grows to zigzag facets, in contrast to the previous model. Such a facet formation process was observed when growth velocity was high, although planar interfaces were maintained throughout crystal growth at low velocities. We theoretically showed that the latent heat of crystallization generates a negative temperature gradient in Si melt and the interface becomes unstable at high growth velocities. When the interface is unstable, the perturbation is amplified and results in zigzag facets.

II. EXPERIMENTAL DETAILS

Figure 1 shows an *in situ* observation system that consists of a furnace and a microscope.²⁰ A Si {100} wafer was set between quartz plates inside the furnace in order to keep the surface of the Si melt flat during crystal growth. Then, the furnace was filled with an ultrahigh-purity argon gas. Subsequently, the Si wafer was heated. There are two heaters in the furnace and thermocouple is located below each heater. Temperature gradient was made in the furnace by setting the temperature of the two heaters at different value. So, melting started from one end of the wafer. Then, furnace temperature was reduced at a steady rate before the complete melting of the wafer, and the shape of the Si crystal-melt interface growing along the [100] direction was observed from the [001] direction. The observation was conducted for various growth velocities by changing cooling rate. After crystallization, we confirmed that the sample was solidified in the [100] direction by crystallographic orientation analysis using the electron backscattering diffraction pattern method.

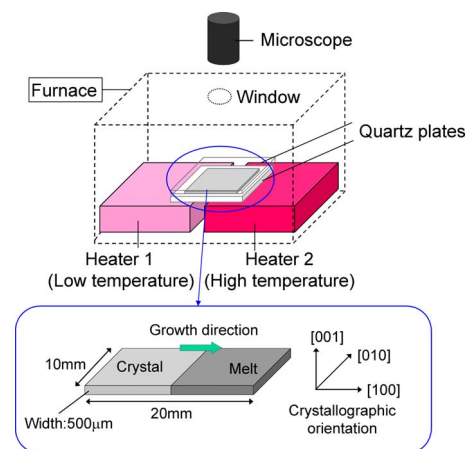


FIG. 1. (Color online) *In situ* observation system that consists of a furnace and a microscope. A Si {100} wafer was set between quartz plates inside the furnace in order to keep the surface of the Si melt flat during crystal growth. There is a temperature gradient in the furnace.

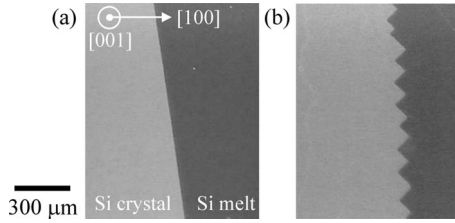


FIG. 2. Si crystal-melt interfaces growing in the [100] direction observed from the [001] direction. The interface moved from left to right in the images. (a) The growth velocity was $123 \mu\text{m/s}$. At this growth velocity, the interface was not faceted and a planar interface was maintained throughout crystal growth. (b) The growth velocity was $147 \mu\text{m/s}$. At this growth velocity, the zigzag faceted interface was observed.

III. RESULTS AND DISCUSSIONS

Figures 2(a) and 2(b) show the Si(100) crystal-melt interfaces whose growth velocities are 123 and $147 \mu\text{m/s}$, respectively. The interface moved from left to right in the images. It should be noted that the interface was not faceted and was macroscopically planar when the growth velocity was $123 \mu\text{m/s}$ and the planar interface was maintained throughout crystal growth. Such a planar interface was observed at lower growth velocities. On the other hand, the zigzag faceted interface was observed when the growth velocity was $147 \mu\text{m/s}$ or higher. Thus, it was shown that the formation of the faceted interface depends on growth velocity.

Next, we investigated the facet formation of the Si(100) crystal-melt interface in more detail. Figure 3(a) shows the shape transition of the interface whose growth velocity is $162 \mu\text{m/s}$. A macroscopically planar interface was observed in the earlier stage of growth. It should be emphasized that a wavy perturbation was introduced into the planar interface, and the perturbation grew and resulted in zigzag facets. Fig-

ure 3(b) shows the isochrones of the interface at $1/6$ s intervals. It should also be noted that the wavelength of the wavy interface completely agreed with that of the zigzag faceted interface. The perturbation was amplified with time and one perturbation peak formed one zigzag facet peak. This facet formation process is different from that predicted using the previous model^{15,16} shown in Fig. 3(c), in which atomic-scale facets are formed first and gradually enlarge to macroscopic facets owing to the loss of short facets. It was directly proved that a wavy perturbation introduced into a planar interface grows to zigzag facets and the scale of the perturbation determines the initial scale of the facets. Williams *et al.*¹⁶ performed scanning electron microscopy observations of recrystallized Si films and observed the remnants of planar and faceted interfaces. They explained that although crystal-melt interfaces were faceted throughout crystal growth, remelting erased the evidence of faceting; thus, the remnants of the planar interface were observed. However, from our results, we consider that they observed the remnants of the shape transition of the growing interface from planar to faceted.

It was clearly shown that the zigzag faceted interface is formed by the amplification of the perturbation introduced into the planar interface when growth velocity is high, although crystals grow with the planar interface at low velocities. Here, we determine why the perturbation is amplified when growth velocity is high, using stability arguments. Since we used high-purity Si wafers in our experiments, we neglect the effect of constitutional supercooling. Therefore, we consider the thermal field of the Si crystal and melt during crystallization along the [100] direction at a constant growth velocity, before the facet formation. In general, a crystal-melt interface becomes unstable, leading to the amplification of the perturbation, when the temperature gradient at the interface is negative along the growth direction.²¹ In this study, the temperature gradient in the furnace was posi-

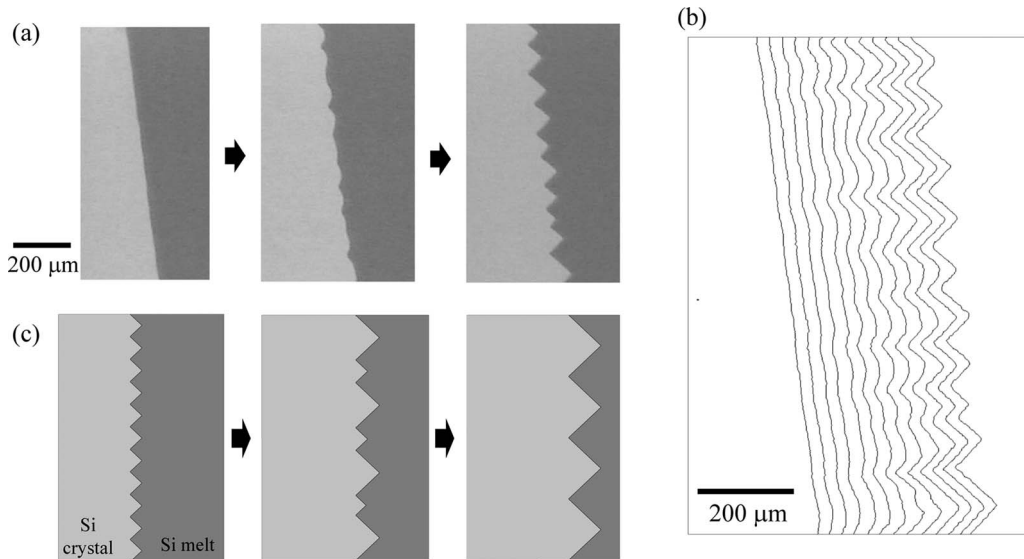


FIG. 3. (a) Shape transition of Si crystal-melt interface. The growth velocity was $162 \mu\text{m/s}$. A macroscopically planar crystal-melt interface was perturbed and resulted in a zigzag faceted interface. (b) Isochrones of interface at $1/6$ s intervals. The wavelength of the perturbation agreed with the facet spacing of the zigzag faceted interface. (c) Concept of previous facet formation model. Atomic-scale facets were gradually enlarged to macroscopic facets owing to the loss of short facets.

tive, initiating crystal growth from a seed crystal. Hence, we consider that the latent heat of crystallization increases the temperature at the crystal-melt interface, and the temperature gradient in the Si melt at the interface becomes negative when growth velocity is high, because the amount of generated latent heat per unit time increases with growth velocity. The thermal field of the Si crystal and melt, $T_{c,m}$, is governed by the partial differential equation²²

$$\begin{aligned} \rho_{c,m} C_{Pc,m} \frac{\partial T_{c,m}}{\partial t} &= -\rho_{c,m} C_{Pc,m} V \frac{\partial T_{c,m}}{\partial x} \\ &= k_{c,m} \frac{\partial^2 T_{c,m}}{\partial x^2} + \frac{2k_q}{l_q l_{Si}} (Gx + T_i - T_{c,m}), \quad (1) \end{aligned}$$

where $\rho_{c,m} C_{Pc,m}$, $k_{c,m}$, k_q , l_q , and l_{Si} are the heat capacity of the Si crystal and melt, the thermal conductivity of the Si crystal and melt, the thermal conductivity of the quartz plate, the thickness of the quartz plate, and the thickness of the Si wafer, respectively. The origin of the coordinate is at the crystal-melt interface, which moves with the growth velocity V . $Gx + T_i$ is the furnace temperature; here, G is the temperature gradient in the furnace and T_i is the furnace temperature at the interface. For simplicity, we assumed that the furnace temperature is temporally constant in considering the inertial system. The first and second terms on the right-hand side of Eq. (1) come from heat diffusion along the growth direction and heat conduction between the Si crystal or melt and the furnace through the quartz plates. The solution of Eq. (1) is

$$T_{c,m} = A_{c,m} \exp\left(-\frac{x}{l_{c,m}}\right) + Gx + \frac{\rho_{c,m} C_{Pc,m} G V l_q l_{Si}}{2k_q} + T_i, \quad (2a)$$

$$l_c = \frac{2}{\rho_c C_{Pc} V / k_c - \sqrt{(\rho_c C_{Pc} V / k_c)^2 + 8k_q / k_c l_q l_{Si}}}, \quad (2b)$$

$$l_m = \frac{2}{\rho_m C_{Pm} V / k_m + \sqrt{(\rho_m C_{Pm} V / k_m)^2 + 8k_q / k_m l_q l_{Si}}}. \quad (2c)$$

Here, $A_{c,m}$ is the constant determined by boundary conditions, namely, the energy conservation at the crystal-melt interface and the temperature continuity at the crystal-melt interface. The former is

$$\Delta H V = k_c \left(\frac{\partial T_c}{\partial x} \right)_{x=0} - k_m \left(\frac{\partial T_m}{\partial x} \right)_{x=0}, \quad (3)$$

where ΔH is the latent heat of Si and the latter is

$$(T_c)_{x=0} = (T_m)_{x=0}. \quad (4)$$

Since the degree of interface undercooling of Si during crystallization in the [100] direction is very small,²³ we can consider that $(T_c)_{x=0} = (T_m)_{x=0} = T_{mp}$, where T_{mp} is the melting point of Si. This relationship determines V for a given furnace temperature.

Figure 4 shows the thermal fields of the Si crystal and melt during crystal growth for $V=50, 123, 147, 200,$ and $250 \mu\text{m/s}$. The physical properties of Si used are based on those indicated in Ref. 24, and l_q , l_{Si} , and G are based on our

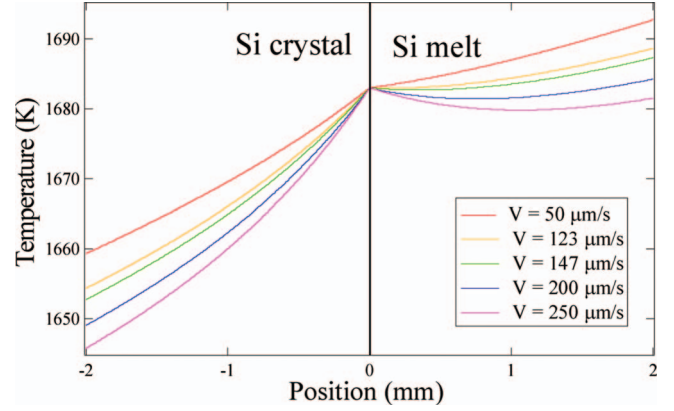


FIG. 4. (Color) Thermal fields of Si crystal and melt during crystallization for $V=50, 123, 147, 200,$ and $250 \mu\text{m/s}$. $\rho_c C_{Pc} = 2.29 \times 10^{-3} \text{ J/mm}^3 \text{ K}$, $\rho_m C_{Pm} = 2.53 \times 10^{-3} \text{ J/mm}^3 \text{ K}$, $k_c = 2.2 \times 10^{-2} \text{ W/mm K}$, $k_m = 5.4 \times 10^{-2} \text{ W/mm K}$, $k_q = 4.3 \times 10^{-3} \text{ W/mm K}$, $l_q = 1.0 \text{ mm}$, $l_{Si} = 0.5 \text{ mm}$, $G = 8 \text{ K/mm}$, $\Delta H = 4.122 \text{ J/mm}^3$, and $T_{mp} = 1683 \text{ K}$. The temperature gradient in the Si melt at the crystal-melt interface changed from positive to negative as V increased.

experimental values. It can be observed in Fig. 4 that the temperature gradient in the Si melt at the interface changes from positive to negative as growth velocity increases. When growth velocity is low, the temperature gradient is positive and the interface is stable. Hence, a planar interface is maintained throughout crystal growth. On the other hand, at high growth velocities, the temperature gradient becomes negative and the perturbation introduced into the planar interface is amplified owing to interface instability and forms zigzag facets. It was proved that the temperature gradient changes from positive to negative as growth velocity increases owing to the latent heat of crystallization, and the faceted interfaces are formed at high growth velocities, because the perturbation grows and results in zigzag facets when the temperature gradient is negative.

The critical growth velocity, at which the temperature gradient changes from positive to negative, calculated using Eq. (1) is $109 \mu\text{m/s}$. On the other hand, the critical growth velocity is between 123 and $147 \mu\text{m/s}$ according to our experimental results. The critical growth velocity predicted by the theory almost agrees with that obtained by experiment and it seems that the theory encapsulates the physical phenomenon under study well. The small disagreement may be caused by the effects that are not contained in Eq. (1). For example, the latent heat of crystallization can be transported by heat radiation. Thus, this effect suppresses the generation of the negative temperature gradient and increases the critical growth velocity.

In Fig. 4, it can be observed that the negative temperature gradient becomes steeper as growth velocity increases. Simultaneously, according to Mullins and Sekerka,²⁵ the wavelength of the perturbation, which is amplified the most, decreases as the negative temperature gradient becomes steeper. Hence, the wavelength of the observed perturbation must decrease with increasing growth velocity if the temperature field shown in Fig. 4 is valid. Then, we investigated the dependence of the wavelength of the wavy perturbation

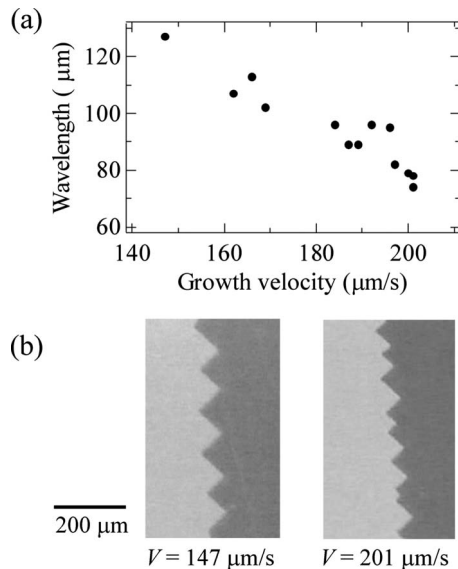


FIG. 5. (a) Dependence of wavelength of perturbed wavy interface on growth velocity. (b) Faceted crystal-melt interfaces immediately after facet formation, whose growth velocities were 147 and 201 $\mu\text{m/s}$. The perturbation wavelength and its corresponding facet wavelength decreased with growth velocity.

on growth velocity. Figure 5(a) shows the dependence of wavelength on growth velocity, and Fig. 5(b) shows the interfaces, immediately after the facet formation, whose growth velocities are 147 and 201 $\mu\text{m/s}$. As predicted,

wavelength decreases as growth velocity increases, and the validity of the dependence of temperature field on growth velocity shown in Fig. 4 was proved. Thus, we can conclude that the latent heat of crystallization generates a negative temperature gradient in the Si melt at high growth velocities, and the negative temperature gradient, which leads to interface instability, is necessary for facet formation.

IV. CONCLUSIONS

We investigated the formation mechanism of a zigzag faceted crystal-melt interface during crystal growth by *in situ* observation. It was directly proved that a wavy perturbation is introduced into a planar crystal-melt interface, and the perturbation is amplified and results in zigzag facets. Faceted interfaces are formed at high growth velocities because the perturbation introduced into a planar interface is amplified when the temperature gradient becomes negative owing to the latent heat of crystallization. The negative temperature gradient, which leads to interface instability, is necessary for facet formation.

ACKNOWLEDGMENTS

This work was partially supported by a Grant-in-Aid for Scientific Research from the Ministry of Education, Culture, Sports, Science and Technology of Japan, and the Global COE Program of the Material Integration International Center of Education and Research of Tohoku University.

*Corresponding author. FAX: +81-22-215-2011; 3gatu3ka@imr.tohoku.ac.jp

¹W. Kurz and D. J. Fisher, *Fundamentals of Solidification*, 4th rev. ed. (Trans Tech, Switzerland, 1998), Chap. 2, Sec. 3.

²I. V. Markov, *Crystal Growth for Beginners*, 2nd ed. (World Scientific, Singapore, 2003), pp. 215–216.

³J. W. Mullin, *Crystallization*, 3rd ed. (Butterworth-Heinemann, Oxford, 1993), pp. 217–218.

⁴K. A. Jackson, *Liquid Metals and Solidification* (American Society for Metals, Cleveland, 1958), p. 174.

⁵K. A. Jackson, *Mater. Sci. Eng.* **65**, 7 (1984).

⁶U. Landman, W. D. Luedtke, R. N. Barnett, C. L. Cleveland, M. W. Ribarsky, E. Arnold, S. Ramesh, H. Baumgart, A. Martinez, and B. Khan, *Phys. Rev. Lett.* **56**, 155 (1986).

⁷U. Landman, W. D. Luedtke, M. W. Ribarsky, R. N. Barnett, and C. L. Cleveland, *Phys. Rev. B* **37**, 4637 (1988).

⁸F. F. Abraham and J. Q. Broughton, *Phys. Rev. Lett.* **56**, 734 (1986).

⁹D. J. Eaglesham, A. E. White, L. C. Feldman, N. Moriya, and D. C. Jacobson, *Phys. Rev. Lett.* **70**, 1643 (1993).

¹⁰K. Fujiwara, K. Nakajima, T. Ujihara, N. Usami, G. Sazaki, H. Hasegawa, S. Mizoguchi, and K. Nakajima, *J. Cryst. Growth* **243**, 275 (2002).

¹¹P. A. Apte and X. C. Zeng, *Appl. Phys. Lett.* **92**, 221903 (2008).

¹²D. Buta, M. Asta, and J. J. Hoyt, *Phys. Rev. E* **78**, 031605 (2008).

¹³M. W. Geis, H. I. Smith, B.-Y. Tsaur, J. C. C. Fan, D. J. Silversmith, and R. W. Mountain, *J. Electrochem. Soc.* **129**, 2812 (1982).

¹⁴M. W. Geis, H. I. Smith, D. J. Silversmith, and R. W. Mountain, *J. Electrochem. Soc.* **130**, 1178 (1983).

¹⁵L. Pfeiffer, S. Paine, G. H. Gilmer, W. van Saarloos, and K. W. West, *Phys. Rev. Lett.* **54**, 1944 (1985).

¹⁶D. A. Williams, R. A. McMahon, and H. Ahmed, *Phys. Rev. B* **39**, 10467 (1989).

¹⁷D. K. Shangguan and J. D. Hunt, *J. Cryst. Growth* **96**, 856 (1989).

¹⁸D. Shangguan and J. D. Hunt, *Metall. Trans. A* **22**, 941 (1991).

¹⁹D. Shangguan and J. D. Hunt, *Metall. Trans. A* **23**, 1111 (1992).

²⁰K. Fujiwara, K. Maeda, N. Usami, and K. Nakajima, *Phys. Rev. Lett.* **101**, 055503 (2008).

²¹W. Kurz and D. J. Fisher, *Fundamentals of Solidification*, 4th rev. ed. (Trans Tech, Switzerland, 1998), p. 45.

²²W. M. Rohsenow, J. P. Hartnett, and E. N. Ganic, *Handbook of Heat Transfer Fundamentals*, 2nd ed. (McGraw-Hill, New York, 1985), Chap. 1.

²³K. M. Beatty and K. A. Jackson, *J. Cryst. Growth* **211**, 13 (2000).

²⁴K.-W. Yi, H.-T. Chung, H.-W. Lee, and J.-K. Yoon, *J. Cryst. Growth* **132**, 451 (1993).

²⁵W. W. Mullins and R. F. Sekerka, *J. Appl. Phys.* **35**, 444 (1964).